

EXTINCTION OF CHOLERA USING DETERMINISTIC AND STOCHASTIC MODELS INCORPORATING VIGILANT HUMAN COMPARTMENT

M. O. ADEWOLE^{1*}, A. I. M. ISMAIL², F. A. ABDULLAH², T. S. FANIRAN³, §

ABSTRACT. We study the effect of vaccination, sanitation and public health sensitization as prevention and control measures of cholera in deterministic and stochastic frameworks. To achieve this, a deterministic mathematical model incorporating the class of vigilant individuals is proposed and analyzed. The results from the stability analysis show that the disease-free equilibrium solution is globally asymptotically stable if $\mathfrak{R}_0 < 1$. The model is then extended to incorporate random effect using the method of transition probabilities. Numerically, we approximate the expected extinction time of the disease if certain conditions are satisfied. As *Vibrio cholerae* multiplies at a fast rate in the environment, it is recommended that regular disinfection of the affected areas as well as public health sensitization be done.

Keywords: Randomness, extinction, intervention, vigilance.

AMS Subject Classification: 92D30, 60J27, 91B70.

1. INTRODUCTION

Cholera, caused by the bacterium *Vibrio cholerae*, is a severe intestinal infectious disease that has remained a serious public health threat in developing countries [1, 2]. It often results in acute diarrhea, vomiting, dehydration and even death (if untreated) [1, 2]. The transmission of cholera involves both direct (i.e., human-to-human) and indirect (i.e., environment-to-human) routes [3]. It mainly spreads by water and food contaminated with human faeces which contain the bacteria [1], contaminated fish and shellfish, or leftover cooked grains that have not been properly reheated [4].

Limitations in monitoring and concerns about the adverse impact on trade and tourism make it difficult to know the exact figure of the incidence of cholera [5]. However, there has been an increasing number of cholera outbreaks worldwide including the large cholera epidemics in Haiti from 2010-2012 with more than 530,000 reported cases and 7000 deaths [6]. Current estimates

¹ Department of Computer Science and Mathematics, Mountain Top University, Prayer City, Ogun State, Nigeria.

e-mail: olamathews@gmail.com; ORCID: <https://orcid.org/0000-0002-9130-6739>.

* Corresponding author.

² School of Mathematical Sciences, Universiti Sains Malaysia, Malaysia.

e-mail: ahmad.izani@usm.my; ORCID: <https://orcid.org/0000-0003-1092-5579>.

e-mail: farahaini@usm.my; ORCID: <https://orcid.org/0000-0002-5215-9617>.

³ Department of Computer Science, Lead City University, Lagos-Ibadan Expressway, Ibadan, Oyo State, Nigeria.

e-mail: tayefaniran@yahoo.com; ORCID: <https://orcid.org/0000-0002-6109-9492>.

§ Manuscript received: July 08, 2021; accepted: November 23, 2021.

TWMS Journal of Applied and Engineering Mathematics, Vol.13, No.3 © Işık University, Department of Mathematics, 2023; all rights reserved.

by World Health Organization show 3 – 5 million cholera cases every year in the world [6, 1]. In 2016, 132,121 cases were reported to WHO from 38 countries. The cases include 2,420 deaths [7]. Although it was classified as a pandemic as of 2010, it is rare in the developed world [1, 4, 5].

Confirmatory test for cholera is by isolating *V. cholerae* from faecal samples and a positive culture test from several patients is required for confirmation of cholera outbreak [1]. Improved sanitation, access to clean water and non-contaminated foods are various ways of preventing cholera [1, 4]. Nelson et al [5] reported that the use of vaccine is not 100% effective. Cholera vaccines are 85% effective for the first six months after vaccination and 50% – 62% during the first year [1, 8, 9]. After two years the level of protection decreases to less than 50% [1]. The primary treatment is rehydration (oral or intravenous) therapy and if the case is severe, antibiotics are included. Zinc supplementation is useful in children [1]. A successfully treated patient is immuned to the disease for a period of time. The mechanism behind this temporary immunity is not known [5].

To understand the mechanisms of the spread of cholera and determination of effective control strategies, several authors have developed mathematical models for the transmission dynamics of the disease. However, cholera models can be deterministic, in which the output of the model is fully determined by the parametric and initial values, or stochastic, where the model possesses some inherent randomness. Deterministic cholera models have been studied by several authors. In [10] the authors introduced a new class of vaccinated people to the model in [11] and incorporated control measures (vaccination, treatment and water sanitation) into the resulting model. The authors then investigated, theoretically, the effect of various intervention approaches on cholera outbreaks and explore optimal strategies for disease control. The results in [10] suggested that different controls interact. Furthermore the costs of controls directly affect the duration and strength of each control in an optimal strategy framework. It was also concluded that better results could be achieved with multiple intervention methods due to the multiple transmission modes of cholera. Beryl et al [12] extended the model proposed by [11] to include the effects of media coverage as intervention strategy. The authors did not consider time-dependent controls in their analysis.

In [13], environment-to-human interaction was only considered whereas in the present study, both environment-to-human and human-to-human interaction are taken into account. Further, in [13], there was no inclusion of a class of vigilant human compartment but this is considered in the present work. In [14], quarantine strategy was considered as an effective treatment to combat cholera but the present study considers two effective preventive classes, namely; vaccinated and vigilant human compartments which are much more effective than quarantine. In [15], the authors formulated an age-structured cholera model with multiple transmissions, saturation incidence and imperfect vaccine but they did not take into account a class of vigilant human compartment, which is considered in the present work. For other works on deterministic cholera model, see [16, 17, 18, 19, 2, 20, 21, 22, 23]. Recently, the effect of non-drug compliance by infected individuals was investigated in [24]. It was reported that while noncompliance to treatment instructions worsens the situation, complying to treatment instructions does not eradicate cholera from a population. Influence of human-to-human transmission route and random effects were not considered in this work.

While deterministic models have been greatly used to further understand the dynamics of the disease, they do not incorporate the effect of environmental fluctuations. In reality, the disease dynamics is exposed to influences that are not completely understood which makes the spread of the disease inherently random. We therefore incorporate stochastic influences into our model. There are several ways to include these fluctuations in the deterministic model. For example, Wang & Wang [25] proposed a deterministic model of two types of vibrios and viruses and further extended the model to include the random effects. Their stochastic model is a system of Markov jump processes that is derived from the dynamics of the deterministic model. They derived a closed-form expression for the disease extinction probability and also validated the analytic estimates with numerical simulations. Their results indicate that there is a sharp threshold which is characterized by the basic reproduction number, R_0 . However, they did not

consider the effect of vaccinated and vigilant human compartments on transmission dynamics of cholera.

Marwa et al [26] developed a stochastic dynamics of cholera epidemic model from deterministic model using two approaches - parameter perturbation method (which involves changing a parameter of interest from the deterministic model to a random variable [27]) and the use transition probabilities. Using a suitable Lyapunov function, stability analysis was carried out for the model obtained by stochastic perturbation method. They gave conditions for global existence, uniqueness of positive solutions, stochastic boundedness, global stability in probability, moment exponential stability and almost sure convergence. They further simulated the sample paths of the stochastic differential equations using the Euler-Maruyama Scheme. [28] investigated the dynamics of cholera using a system of stochastic differential equations. It was assumed that the environmental noise is proportional to the variables (which leads to the introduction of new parameters whose values were assumed) and established sufficient conditions for extinction of the disease. By constructing a suitable stochastic Lyapunov function, sufficient criteria that guarantee the existence of a unique ergodic stationary distribution of the positive solutions to the model was given.

In this work, our focus is to study the effect of vaccination, sanitation and public health sensitization as prevention and control measures of cholera in deterministic and stochastic frameworks. Can these control measures lead to the extinction of cholera in the presence of uncertainties? To answer this question and to give more insight into the dynamics of cholera, a stochastic model for cholera transmission which incorporates the two most effective preventive classes-the vaccinated (those who are immunized against cholera) and vigilant (those who adhere to the cholera control measures of the World Health Organization) compartments into human population is presented. First, a deterministic mathematical model is formulated and extended (using the approach in [29, Section 5.6]) to include stochastic influences. The advantage of the modeling procedure used for our stochastic model is that the diffusion coefficients depend on the parameters derived from the basic assumptions of the model. This gives a better understanding of the how the parameters influence the stochastic nature of the system. The models are shown to have a unique solution and sufficient conditions that guarantee the extinction of the disease in an endemic setting are given. Numerically, we approximate the expected extinction time of the disease if certain conditions are satisfied. As *Vibrio cholerae* multiplies at a fast rate in the environment, it is recommended that regular disinfection of the affected areas as well as public health sensitization be done.

The remaining parts of this paper are organized as follows: In Section 2, a deterministic model is formulated and its stationary solutions are analyzed. In Section 3, we incorporate random effect into the deterministic model and establish global existence as well as uniqueness of positive solutions of the new model. Section 4 presents a detailed discussion of results and Section 5 presents the conclusion.

2. MODEL DEVELOPMENT

2.1. Deterministic Model. We propose a deterministic model where the human population is divided into four compartments: susceptible human S , infected human I , vaccinated human V_a and vigilante human V_i . We denote by B , the concentration of vibrios in the environment. As in [30], it is assumed that bacteria enter the aquatic reservoir of *V. cholerae* at a logistic per-biomass rate $\rho \left(1 - \frac{B(t)}{K_B}\right)$ proportional to bacteria density and leaves at a rate $(\tau + \sigma)B$. Here $\rho > 0$ is the per capita growth rate for *V. cholerae*, $K_B > 0$ is the environmental carrying capacity for *V. cholerae* per ml in the water supply. σ is the decay rate of vibrios while τ represent the disinfection rate. We further assumed that a single use of disinfectant can be effective for a period of ϖ . The human recruitment rate is assumed constant (Λ) and that the newly recruited individuals are without cholera.

Susceptible individuals could contract vibrio cholera through interaction with infected individuals at a rate $\alpha_h(1 - \delta)I$ and also contact it from the environment with incidence term $\alpha_e \frac{B}{K+B}$. Parameter α_h is susceptible-infected individual interaction rate while α_e is the interaction rate

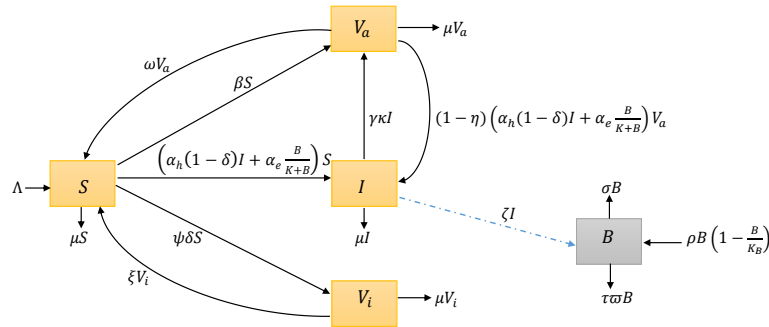


FIGURE 1. Cholera transmission diagram.

between susceptible individuals and vibrio cholerae bacteria in the environment. \mathcal{K} is the half saturation concentration of environmental vibrios and δ is the efficacy of public health sensitization. Susceptible individuals are vaccinated at a constant rate β and as there is no permanent immunity against cholera [1, 8, 5, 9], vaccinated individual lose immunity and become susceptible at the rate ω . It is assumed that the vaccine may fail with failure rate $(1 - \eta)$, where η represents vaccine efficacy. The infected population diminishes through natural death rate μ and recovery (due to treatment) rate $\gamma\kappa$. It is assumed that a successfully treated individual is vaccinated. The susceptible individuals are educated and become vigilant at the rate ψ , but vigilant individuals may become careless in following the precautions at the rate ξ . It is assumed that vigilant individuals don't contract the disease unless they become susceptible.

Based on the aforementioned dynamics, the flowchart schema showing the transmission process of cholera is shown in Fig. 1. The meanings of the parameters are given in Table 1. Cholera-induced mortality is neglected because fatality rates for cholera are very low in general (1,304 deaths out of 172,454 cases in 2015 [1]). The dynamics of the transmission can therefore be described by the following system of ordinary differential equations:

$$\frac{dS}{dt} = \Lambda - \left(\alpha_h(1 - \delta)I + \alpha_e \frac{B}{\mathcal{K} + B} \right) S - (\mu + \beta + \delta\psi)S + \omega V_a + \xi V_i, \tag{1}$$

$$\frac{dI}{dt} = \left(\alpha_h(1 - \delta)I + \alpha_e \frac{B}{\mathcal{K} + B} \right) ((1 - \eta)V_a + S) - (\mu + \gamma\kappa)I, \tag{2}$$

$$\frac{dV_a}{dt} = \beta S + \gamma\kappa I - (\omega + \mu)V_a - (1 - \eta) \left(\alpha_h(1 - \delta)I + \alpha_e \frac{B}{\mathcal{K} + B} \right) V_a, \tag{3}$$

$$\frac{dV_i}{dt} = \psi\delta S - (\xi + \mu)V_i, \tag{4}$$

$$\frac{dB}{dt} = \rho \left(1 - \frac{B}{K_B} \right) B + \zeta I - \sigma B - \tau\omega B. \tag{5}$$

The total human population $N(t) = S(t) + I(t) + V_a(t) + V_i(t)$. If $N(0) = N_0$, then from (1)–(4), we have

$$N(t) = \frac{\Lambda}{\mu} + \left(N_0 - \frac{\Lambda}{\mu} \right) \exp(-\mu t). \tag{6}$$

The following obvious result gives the feasible region of equations (1)–(5):

Theorem 2.1. *Let the initial data for the cholera model (1)–(5) be $S(0) > 0$, $I(0) \geq 0$, $V_a(0) \geq 0$, $V_i \geq 0$ and $B(0) > 0$. Then the solutions $(S(t), I(t), V_a(t), V_i(t), B(t))$ of the model will remain non-negative for all time $t > 0$. Furthermore if $S(0) + I(0) + V_a(0) + V_i(0) \leq \frac{\Lambda}{\mu}$ and $B(0) \leq K_B$, then the feasible region of solution is defined by*

$$\Gamma = \left\{ (S(t), I(t), V_a(t), V_i(t), B(t)) \in \mathbb{R}_+^4 \times \mathbb{R}_+ : S(t) + I(t) + V_a(t) + V_i(t) \leq \frac{\Lambda}{\mu}, B(t) \leq M \right\},$$

TABLE 1. Summary of the parameters

Parameter	Meaning	Value	Reference
μ	Natural human death rate	$(43.5 \text{ year})^{-1}$	[31]
α_h	Human-to-human transmission rate	0.00011 day^{-1}	[11]
α_e	Environment-to-human transmission rate	0.075 day^{-1}	[11]
τ	Disinfection rate	4 year^{-1}	[2]
ϖ	Duration of effectiveness of disinfection	14 days	Assumed
K_B	Environmental carrying capacity for <i>V. cholerae</i>	$10^9 / \text{ml}$	[32]
ρ	per capita growth rate for <i>V. cholerae</i>	0.73 day^{-1}	[33]
σ	Decay rate of vibrios	30^{-1} day^{-1}	[34]
ω	Loss of immunity rate	0.03417 day^{-1}	Calculated
ζ	Rate of human contribution to vibrios	10 cells/ml-day	[34]
γ	Recovery rate	0.2 day^{-1}	[34]
Λ	Human recruitment rate	30 people per year	Assumed
β	Vaccination rate	4 year^{-1}	Assumed
η	Vaccine efficacy	0.8	Assumed
δ	Efficacy of public health sensitization	$0 < \delta < 1$	
\mathcal{K}	half saturation concentration of environmental vibrios	10^6 cells/ml	[33]
ξ	Loss of vigilance rate	0.2 day^{-1}	Assumed
ψ	Vigilance rate	0.6 day^{-1}	Assumed
κ	Drug/treatment efficacy	$0 < \kappa < 1$	

where

$$M = \frac{1}{2\rho} \left(K_B(\rho - \sigma - \tau\varpi) + \sqrt{K_B^2(\rho - \sigma - \tau)^2 + 4\rho\zeta K_B \frac{\Lambda}{\mu}} \right).$$

System (1)–(5) has a disease-free equilibrium (DFE) given by

$$\varepsilon_0 = (S^*, I^*, V_a^*, V_i^*, B^*) = \left(\frac{\Lambda(\xi + \mu)(\omega + \mu)}{\mu\chi}, 0, \frac{\Lambda\beta(\xi + \mu)}{\mu\chi}, \frac{\Lambda\psi\delta(\omega + \mu)}{\mu\chi}, 0 \right), \tag{7}$$

where $\chi = \beta(\xi + \mu) + (\omega + \mu)(\mu + \xi + \psi\delta)$. Using the next generation operator approach of [35], the basic reproduction number, associated with DFE ε_0 and denoted by \mathfrak{R}_0 is obtained as

$$\mathfrak{R}_0 = \frac{1}{2}\mathcal{U} + \frac{1}{2}\sqrt{\mathcal{U}^2 - \frac{4\alpha_h(1 - \delta)\rho(S^* + (1 - \eta)V_a^*)}{(\gamma\kappa + \mu)(\sigma + \tau\varpi)}}, \tag{8}$$

where

$$\mathcal{U} = \frac{\rho}{\sigma + \tau\varpi} + \frac{(S^* + (1 - \eta)V_a^*)\alpha_h(1 - \delta)}{\gamma\kappa + \mu} + \frac{(S^* + (1 - \eta)V_a^*)\alpha_e\zeta}{\mathcal{K}(\gamma\kappa + \mu)(\sigma + \tau\varpi)}.$$

The basic reproduction number \mathfrak{R}_0 is a measure of the average number of new infections generated by a single infected person during the person’s infectious period in a population that is fully susceptible [35]. For simplicity, we define

$$\mathfrak{R}_1 = \frac{\rho}{\sigma + \tau\varpi} + \frac{(S^* + (1 - \eta)V_a^*)\alpha_h(1 - \delta)}{\gamma\kappa + \mu} + \frac{(S^* + (1 - \eta)V_a^*)\alpha_e\zeta}{\mathcal{K}(\gamma\kappa + \mu)(\sigma + \tau\varpi)} - \frac{(S^* + (1 - \eta)V_a^*)\rho\alpha_h(1 - \delta)}{(\gamma\kappa + \mu)(\sigma + \tau\varpi)}.$$

It is easy to see that

$$\mathfrak{R}_0 < 1 \Leftrightarrow \mathfrak{R}_1 < 1, \quad \mathfrak{R}_0 = 1 \Leftrightarrow \mathfrak{R}_1 = 1, \quad \mathfrak{R}_0 > 1 \Leftrightarrow \mathfrak{R}_1 > 1, \tag{9}$$

2.2. Stability Analysis. Nonlinear models such as (1)–(5) exhibit complex population dynamics and possess delicate exchange of stability properties. As basic reproduction number \mathfrak{R}_0 needs fall below unity to eliminate a disease, it becomes important to investigate the stability of equilibrium solutions when $\mathfrak{R}_0 < 1$.

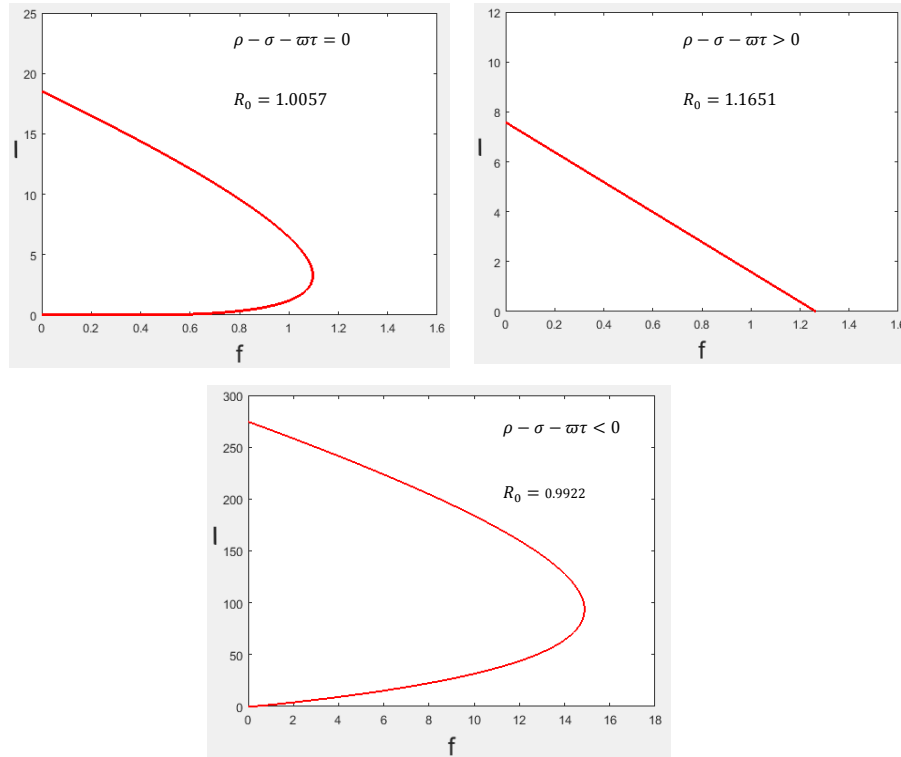


FIGURE 2. Diagram showing that the number of equilibrium points changes with changes in $(\rho - \sigma - \tau\omega)$. The parameter values in Table 1 are used with τ chosen such that each condition is met.

Let $\varepsilon_1 = (S^*, I^*, V_a^*, V_i^*, B^*)$ be an arbitrary equilibrium of (1)–(5). We set the right side of (1)–(5) to zero and solve the resulting equations to obtain

$$\begin{aligned}
 B^* &= \frac{K_B(\rho - \tau\omega - \sigma) + \sqrt{K_B^2(\rho - \tau\omega - \sigma)^2 + 4\rho K_B \zeta I^*}}{2\rho} \\
 S^* &= \frac{\Lambda c_3 \left[\left(\alpha_h(1 - \delta)I^* + \frac{\alpha_e B^*}{\mathcal{K} + B^*} \right) + \mu + \omega \right] + \kappa\gamma\omega I^*}{\left[(1 - \eta) \left(\alpha_h(1 - \delta)I^* + \frac{\alpha_e B^*}{\mathcal{K} + B^*} \right) + \mu + \omega \right] \left[\left(\left(\alpha_h(1 - \delta)I^* + \frac{\alpha_e B^*}{\mathcal{K} + B^*} \right) + c_2 \right) c_3 - \psi\xi \right] - \omega\beta c_3} \\
 V_a^* &= \frac{\kappa\gamma\xi I^* - \kappa\gamma c_3 I^* \left[\left(\alpha_h(1 - \delta)I^* + \frac{\alpha_e B^*}{\mathcal{K} + B^*} \right) + c_2 \right] + \Lambda\beta c_3}{\left[(1 - \eta) \left(\alpha_h(1 - \delta)I^* + \frac{\alpha_e B^*}{\mathcal{K} + B^*} \right) + \mu + \omega \right] \left[\left(\left(\alpha_h(1 - \delta)I^* + \frac{\alpha_e B^*}{\mathcal{K} + B^*} \right) + c_2 \right) c_3 - \psi\xi \right] - \omega\beta c_3} \\
 V_i^* &= \frac{\psi \left[(1 - \delta) \left(\alpha_h(1 - \delta)I^* + \frac{\alpha_e B^*}{\mathcal{K} + B^*} \right) + \Lambda(\mu + \omega) - \kappa\gamma\omega I^* \right]}{\left[(1 - \eta) \left(\alpha_h(1 - \delta)I^* + \frac{\alpha_e B^*}{\mathcal{K} + B^*} \right) + \mu + \omega \right] \left[\left(\left(\alpha_h(1 - \delta)I^* + \frac{\alpha_e B^*}{\mathcal{K} + B^*} \right) + c_2 \right) c_3 - \psi\xi \right] - \omega\beta c_3},
 \end{aligned}$$

and I^* can be obtained by solving

$$f(I^*) = \left(\alpha_h(1 - \delta)I^* + \alpha_e \frac{B^*}{\mathcal{K} + B^*} \right) \left((1 - \eta)V_a^* + S^* \right) - (\mu + \gamma\kappa)I^* = 0, \tag{10}$$

where

$$c_2 = \mu + \beta + \psi, \quad c_3 = \xi + \mu.$$

Finding exact solution to (10) is somewhat difficult, we therefore employ numerical means. The nature of $(\rho - \sigma - \tau\omega)$ has great influence on the number of equilibrium points and their stability. This is shown in Figure 2.

It is clear from (8) that $\frac{\rho}{\tau\omega + \sigma} < 1$ for \mathfrak{R}_0 to be less than unity. It therefore implies that disinfection of the water body and other cholera affected areas is necessary for cholera eradication

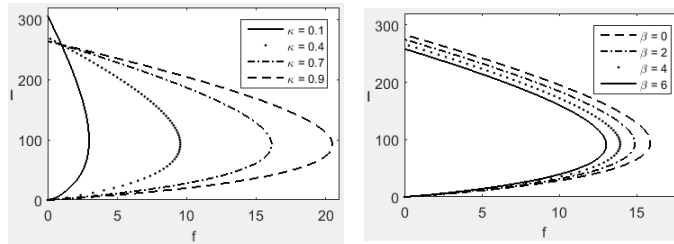


FIGURE 3. Diagram showing the influence of κ and β on the number of equilibrium when $\rho - \sigma - \tau\varpi < 0$. The parameter values in Table 1 are used.

and control. Figure 3 shows that treatment efficacy κ and public health sensitization β do not affect the number of stationary points when $\rho - \sigma - \tau\varpi < 0$.

It has been seen in Figure 2 that two equilibrium points are obtainable when $\mathfrak{R}_0 < 1$. Next we justify that the disease-free equilibrium is the stable equilibrium when $\mathfrak{R}_0 < 1$.

Following the local stability result of [36], we have

Theorem 2.2. *The disease-free equilibrium ε_0 of (1)–(5) is locally asymptotically stable in Γ if $\mathfrak{R}_0 < 1$.*

For the global asymptotic stability of the disease free equilibrium, we need the following result introduced by Castillo-Chavez et al [37] and has been used in [38].

Lemma 2.1. *Consider a model system written in the form*

$$\begin{aligned} \frac{dX}{dt} &= F(X, Y), \\ \frac{dY}{dt} &= G(X, Y), \quad G(X, 0) = 0, \end{aligned}$$

where $X \in \mathbb{R}^m$ denotes (its components) the number of uninfected individuals and $Y \in \mathbb{R}^n$ denotes (its components) the number of infected individuals. $(X^*, 0)$ denotes the disease-free equilibrium of the system.

Also assume the conditions (C1) and (C2) below:

C1: For $\frac{dX}{dt} = F(X, 0)$, X^* is globally asymptotically stable;

C2: $G(X, Y) = AY - \tilde{G}(X, Y)$, $\tilde{G}(X, Y) \geq 0$ for $(X, Y) \in \Gamma$, where the Jacobian $A = \frac{\partial G}{\partial Y}(X^*, 0)$ is an M-matrix (whose off-diagonal elements are non-negative) and Γ is the region where the model makes biological sense.

Then the DFE $(X^*, 0)$ is globally asymptotically stable provided that $\mathfrak{R}_0 < 1$.

Theorem 2.3. *The disease-free equilibrium ε_0 of (1)–(5) is globally asymptotically stable in Γ if $\mathfrak{R}_0 < 1$ and unstable if $\mathfrak{R}_0 > 1$.*

Proof. From (1)–(5),

$$\begin{aligned} F(X, Y) &= \begin{bmatrix} \Lambda - \left(\alpha_h(1 - \delta)I + \alpha_e \frac{B}{\mathcal{K} + B}\right) S - (\mu + \beta + \delta\psi)S + \omega V_a + \xi V_i \\ \beta S + \gamma\kappa I - (\omega + \mu)V_a - (1 - \eta) \left(\alpha_h(1 - \delta)I + \alpha_e \frac{B}{\mathcal{K} + B}\right) V_a \\ \psi\delta S - (\xi + \mu)V_i \end{bmatrix}, \\ G(X, Y) &= \begin{bmatrix} \left(\alpha_h(1 - \delta)I + \alpha_e \frac{B}{\mathcal{K} + B}\right) ((1 - \eta)V_a + S) - (\mu + \gamma\kappa)I \\ \rho \left(1 - \frac{B}{\mathcal{K} + B}\right) B + \zeta I - \sigma B - \tau\varpi B \end{bmatrix}. \end{aligned}$$

Condition (C1) is satisfied. To see this, observe that

$$\frac{dX}{dt} = \begin{bmatrix} \Lambda - (\mu + \beta + \delta\psi)S + \omega V_a + \xi V_i \\ \beta S - (\omega + \mu)V_a \\ \psi\delta S - (\xi + \mu)V_i \end{bmatrix}. \tag{11}$$

The Jacobian matrix of (11) is

$$J_X = \begin{bmatrix} -(\mu + \beta + \delta\psi) & \omega & \xi \\ \beta & -(\omega + \mu) & 0 \\ \psi\delta & 0 & -(\xi + \mu) \end{bmatrix},$$

and the eigenvalues are

$$\Delta = \begin{bmatrix} -\mu & \\ -\frac{1}{2}(\delta\psi + \beta + \mu + \omega + \xi) - \frac{1}{2}\sqrt{\Pi_1} & \\ -\frac{1}{2}(\delta\psi + \beta + \mu + \omega + \xi) + \frac{1}{2}\sqrt{\Pi_1} & \end{bmatrix},$$

which all have negative real parts. Where

$$\Pi_1 = \delta^2\psi^2 + 2\beta\delta\psi - 2\delta\psi\omega + 2\delta\psi\xi + \beta^2 + 2\beta\omega - 2\beta\xi + \omega^2 - 2\omega\xi + \xi^2$$

and

$$\begin{aligned} \Pi_2 = & (\gamma\kappa + \mu + \rho - \sigma - \tau\varpi)^2 + ((1 - \eta)V_a^* + S^*)^2\alpha_h^2(1 - \delta)^2 \\ & - 2((1 - \eta)V_a^* + S^*)\alpha_h(1 - \delta)(\gamma\kappa + \mu + \rho - \sigma - \tau\varpi) + \frac{1}{\mathcal{K}}((1 - \eta)V_a^* + S^*)\zeta\alpha_e. \end{aligned}$$

To verify condition (C2), we obtain

$$A = \begin{bmatrix} \alpha_h(1 - \delta)(S^* + (1 - \eta)V_a^*) - (\mu + \gamma\kappa) & \frac{\alpha_e}{\mathcal{K}}(S^* + (1 - \eta)V_a^*) \\ \zeta & \rho - \sigma - \tau\varpi \end{bmatrix}.$$

Then

$$\tilde{G}(X, Y) = \begin{bmatrix} [S^* + (1 - \eta)V_a^* - (S + (1 - \eta)V_a)]\alpha_h(1 - \delta)I + \alpha_e B \left[S^* + (1 - \eta)V_a^* - \frac{S + (1 - \eta)V_a}{B + \mathcal{K}} \right] \\ \frac{\rho B^2}{K_B} \end{bmatrix}.$$

It is not difficult to see from (7) and Theorem 2.1 that $\tilde{G}(X, Y) \geq 0$ for $(X, Y) \in \Gamma$. Therefore based on Lemma 2.1, the DFE ε_0 is globally asymptotically stable when $\mathfrak{R}_0 < 1$. \square

The epidemiological implication of Theorems 2.2 and 2.3 is that there is no possibility of backward bifurcation. Therefore, the requirement of the reproduction number to be less than one is a sufficient condition for cholera control and elimination.

3. STOCHASTIC MODEL

In this section we formulate a system of stochastic differential equations (SDEs) from the deterministic model (1)–(5) using the method of transition probabilities [29, 39]. This method produces Itô stochastic differential equation model. Let $X(t)$ be a d -dimensional column vector and \mathcal{W}_t be an m -dimensional column vector of independent Wiener processes. The SDE takes the form

$$dX(t) = f(X, t) dt + G(X, t) d\mathcal{W}_t \quad \text{for } t \geq t_0, \tag{12}$$

with initial value $X(0) = X_0 \in \mathbb{R}^d$ where $f(X, t)$ is a d -dimensional column vector and $G(X, t)$ is $d \times m$ matrix.

After considering the transition probabilities, we obtain (see Appendix A for details)

$$\begin{pmatrix} dS \\ dI \\ dV_a \\ dV_1 \\ dB \end{pmatrix} = \begin{pmatrix} \Lambda - \Theta_1 S - (\mu + \beta + \psi)S + \omega V_a + \xi V_i \\ \Theta_1((1 - \eta)V_a + S) - (\mu + \gamma\kappa)I \\ \beta S + \gamma\kappa I - (\omega + \mu)V_a - (1 - \eta)\Theta_1 V_a \\ \psi S - (\xi + \mu)V_i \\ \rho \left(1 - \frac{B}{K_B}\right) B + \zeta I - \sigma B - \tau\varpi B \end{pmatrix} dt$$

$$+ \begin{pmatrix} \sqrt{\Lambda} & 0 & 0 & 0 & 0 \\ -\sqrt{\Theta_1 S} & \sqrt{\Theta_1 S} & 0 & 0 & 0 \\ -\sqrt{\mu S} & -\sqrt{\mu I} & -\sqrt{\mu V_a} & -\sqrt{\mu V_i} & 0 \\ -\sqrt{\beta S} & 0 & \sqrt{\beta S} & 0 & 0 \\ -\sqrt{\psi \delta S} & 0 & 0 & \sqrt{\psi \delta S} & 0 \\ \sqrt{\omega V_a} & 0 & -\sqrt{\omega V_a} & 0 & 0 \\ \sqrt{\xi V_i} & 0 & 0 & -\sqrt{\xi V_i} & 0 \\ 0 & \sqrt{\Theta_1(1-\eta)V_a} & -\sqrt{\Theta_1(1-\eta)V_a} & 0 & 0 \\ 0 & -\sqrt{\gamma \kappa I} & \sqrt{\gamma \kappa I} & 0 & 0 \end{pmatrix}^T \begin{pmatrix} dW_t^1 \\ dW_t^2 \\ dW_t^3 \\ dW_t^4 \\ dW_t^5 \\ dW_t^6 \\ dW_t^7 \\ dW_t^8 \\ dW_t^9 \end{pmatrix} \tag{13}$$

where

$$\Theta_1 = \left(\alpha_h(1 - \delta)I + \alpha_e \frac{B}{\mathcal{K} + B} \right).$$

We do not consider $B(t)$ in the formulation of transitions because there is no transition from human population to Vibrios and vice versa.

To provide the appropriate framework, we give some notations and results on Itô SDEs contained in [40]. $(\Omega, \mathcal{F}, \{\mathcal{F}_t\}_{t \geq 0}, \mathbb{P})$ denotes a complete probability space. $\{\mathcal{F}_t\}_{t \geq 0}$ is an increasing and right continuous filtration while $\{\mathcal{F}_0\}$ contains all \mathbb{P} -null sets. The following spaces will be needed

$$\begin{aligned} \mathbb{R}_+^d &= \{x = (x_1, x_2, \dots, x_d) \in \mathbb{R}^d : x_i > 0, i = 1, 2, \dots, d\} \\ \bar{\mathbb{R}}_+^d &= \{x = (x_1, x_2, \dots, x_d) \in \mathbb{R}^d : x_i \geq 0, i = 1, 2, \dots, d\}. \end{aligned}$$

\mathcal{W}_t denotes an m -dimensional Wiener process defined the complete probability space $(\Omega, \mathcal{F}, \{\mathcal{F}_t\}_{t \geq 0}, \mathbb{P})$.

3.1. Existence and Uniqueness of Positive Solution. In the study of the dynamics of an epidemic model and to investigate the long-term behaviour the model, justification of the existence of a unique global positive solution is important. We therefore have the following:

Theorem 3.1. *Given an initial value $X_0 = (S_0, I_0, V_{a0}, V_{i0}, B_0) \in \mathbb{R}_+^5$, there exists a unique positive solution $X(t) = (S(t), I(t), V_a(t), V_i(t), B(t))$ of system (13) on $t \geq 0$ and the solution will remain in \mathbb{R}_+^5 with probability one.*

Proof.

$$f(S_1, I, V_a, V_i, B) - f(S_2, I, V_a, V_i, B) = \begin{pmatrix} -\Theta_2(S_1 - S_2) \\ \Theta_1(S_1 - S_2) \\ \beta(S_1 - S_2) \\ \psi(S_1 - S_2) \\ 0 \end{pmatrix}$$

where $\Theta_2 = \Theta_1 + \mu + \beta + \psi$.

$$\begin{aligned} |f(S_1, I, V_a, V_i, B) - f(S_2, I, V_a, V_i, B)| &= \sqrt{\Theta_1^2 + \Theta_2^2 + \beta^2 + \psi^2} |S_1 - S_2| \\ &\leq K_{\text{local}}^1 |S_1 - S_2|. \end{aligned}$$

This shows that f is locally Lipschitz continuous with respect to S . By a similar calculation, one can see that f is locally Lipschitz continuous with respect to I, V_a, V_i and B .

Let $\Pi = G(S_1, I, V_a, V_i, B) - G(S_2, I, V_a, V_i, B)$, then

$$\begin{aligned} |\Pi| &= \sqrt{\Pi^T \Pi} \\ &= \left(2 \left(\sqrt{\Theta_1 S_1} - \sqrt{\Theta_1 S_2} \right)^2 + 2 \left(\sqrt{\beta S_1} - \sqrt{\beta S_2} \right)^2 \right. \\ &\quad \left. + 2 \left(\sqrt{\psi S_1} - \sqrt{\psi S_2} \right)^2 + \left(\sqrt{\mu S_1} - \sqrt{\mu S_2} \right)^2 \right)^{1/2} \\ &\leq \sqrt{2} (\Theta_1 + \beta + \psi + \mu)^{1/2} (\sqrt{S_1} - \sqrt{S_2}) = \frac{\sqrt{2} (\Theta_1 + \beta + \psi + \mu)^{1/2}}{(\sqrt{S_1} + \sqrt{S_2})} |S_1 - S_2| \\ &\leq K_{\text{local}}^2 |S_1 - S_2| \end{aligned}$$

This shows that G is locally Lipschitz continuous with respect to S . By a similar calculation, one can see that G is locally Lipschitz continuous with respect to I, V_a, V_i and B .

Now

$$\begin{aligned} X^T f(X, t) + \frac{1}{2} |G(X, t)|^2 &= S \left(\Lambda - \left(\alpha_h I + \alpha_e \frac{B}{\mathcal{K} + B} \right) S - (\mu + \beta + \psi) S + \omega V_a + \xi V_i \right) \\ &\quad + I \left(\left(\alpha_h I + \alpha_e \frac{B}{\mathcal{K} + B} \right) ((1 - \eta) V_a + S) - (\mu + \gamma \kappa) I \right) \\ &\quad + V_a \left(\beta S + \gamma \kappa I - (\omega + \mu) V_a - (1 - \eta) \left(\alpha_h I + \alpha_e \frac{B}{\mathcal{K} + B} \right) V_a \right) \\ &\quad + V_i (\psi S - (\xi + \mu) V_i) + B \left(\rho \left(1 - \frac{B}{K_B} \right) B + \zeta I - \sigma B - \tau \varpi B \right) \\ &\quad + \frac{1}{2} \Lambda + \left(\alpha_h I + \alpha_e \frac{B}{\mathcal{K} + B} \right) ((1 - \eta) V_a + S) + (\beta + \psi) S + \omega V_a \\ &\quad + \xi V_i + \gamma \kappa I + \frac{1}{2} \mu (S + I + V_a + V_i). \end{aligned}$$

Using Young's inequality together with the fact that $\frac{B}{\mathcal{K} + B} < 1$ and $\left(1 - \frac{B}{K_B} \right) < 1$, we obtain

$$X^T f(X, t) + \frac{1}{2} |G(X, t)|^2 \leq c_1 + c_2 S^2 + c_3 I^2 + c_4 V_a^2 + c_5 V_i^2 + c_6 B^2,$$

where

$$\begin{aligned} c_1 &= \frac{1}{2} \left(2\Lambda + \alpha_e (2 - \eta) + \beta + 2\gamma \kappa + \omega + \xi + \frac{1}{4} \mu \right), \\ c_2 &= \frac{1}{4} (2\Lambda + 8\Theta_1 + \omega + \xi - 2\mu + 2\alpha_e + 2\alpha_h + 2\beta + 2\gamma \kappa), \\ c_3 &= \frac{1}{2} ((\alpha_h + \Theta_1)(2 - \eta) + \gamma \kappa + \zeta - \mu), \\ c_4 &= \frac{1}{4} (2(\alpha_h + \alpha_e + 3\Theta_1)(2 - \eta) + 2\omega - 2\mu + \beta + \gamma \kappa), \\ c_5 &= \frac{1}{4} (\psi - 2\mu + 2\xi), \quad c_6 = \rho + \frac{\zeta}{2} - \sigma - \tau \varpi. \end{aligned}$$

For every $T > 0$, there exists $K_T = \max\{c_1, c_2, c_3, c_4, c_5, c_6\}$ such that

$$X^T f(X, t) + \frac{1}{2} |G(X, t)|^2 \leq K_T (1 + S^2 + I^2 + V_a^2 + V_i^2 + B^2).$$

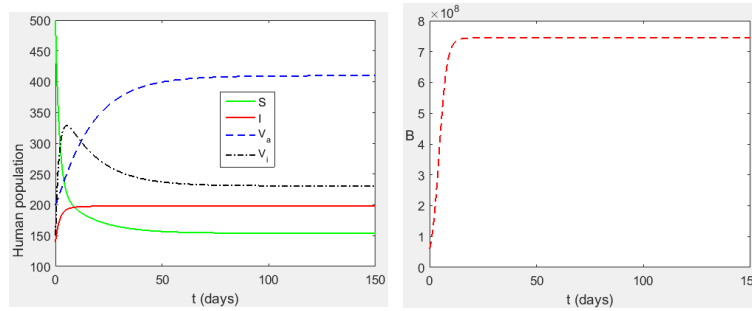


FIGURE 4. Simulation of model (1)–(5) using the parameter values in Table 1

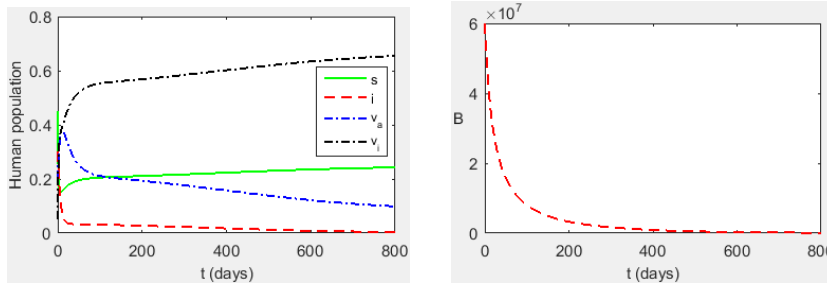


FIGURE 5. Simulation of model (1)–(5) taking $\tau = 18.3$, $\delta = 0.9$ and $\alpha_e = 0.025$ such that $\mathfrak{R}_0 = 0.9935$. Other parameter values are as contained in Table 1.
 $s = \frac{S(t)}{N(t)}$, $i = \frac{I(t)}{N(t)}$, $v_a = \frac{V_a(t)}{N(t)}$, $v_i = \frac{V_i(t)}{N(t)}$,

It follows from [40, Theorem 3.6, page 58] that (13) has a unique global solution. The non-negativity of the solution is similar to Khan et al. [41, Theorem 4.2] and therefore omitted here. This completes the proof. \square

4. DISCUSSION OF RESULTS

4.1. Deterministic Model. System (1)–(5) is solved on MATLAB platform using fourth order Runge-Kutta scheme for system of ordinary differential equations. Parameter values in Table 1 with initial values $S_h(0) = 0.45N_0$, $i_h(0) = 0.3N_0$, $V_a(0) = 0.2N_0$, $V_i(0) = 0.05N_0$, $B(0) = 6 \times 10^7$ are used for the simulation. Figure 4 shows the disease is endemic if $\mathfrak{R}_0 > 1$.

The DFE is globally asymptotically stable therefore the possibility of backward bifurcation in the dynamics of the disease is ruled out. Thus, the condition $\mathfrak{R}_0 < 1$ is sufficient for cholera eradication. It is obvious that a change in vaccination rate does not result to a change in the value of \mathfrak{R}_0 . Therefore vaccination of susceptible individuals can not lead to the eradication of cholera. As strategies of intervention, we consider (i) increase in disinfection rate (τ), (ii) improvement in public health education (δ) and (iii) provision of safe drinking water to reduce environment-to-human transmission rate (α_e). Figure 5 shows that with appropriate choices of τ , δ and α_e such that $\mathfrak{R}_0 < 1$, the disease can be eradicated. This is because the condition $\mathfrak{R}_0 < 1$ is sufficient for the disease eradication (see Theorem 2.3). Also at the initial stage in Figure 5, the number of vaccinated individuals increases but later decreases. This suggests that the cost or burden of vaccination will reduce with time if public health sensitization is effective, regular disinfection of contaminated areas is done and human contribution to *V. cholerae* in the environment is greatly reduced by having a safe place for defecation.

We choose τ, δ, α_e such that $\mathfrak{R}_0 < 1$ in Figure 6. The graphs confirm Theorem 2.3 as it can be seen that $(I, B) \rightarrow (0, 0)$. It is also seen that convergence to zero of the disease classes is fastest with the combination of the three interventions.

Hartley et al. [42] reported that the interactions between the host, *V. cholerae* and environment are associated with the seasonal epidemics of cholera seen in endemic regions. Next, we investigate, numerically, the effects of seasonal variation on the disease dynamics. Seasonality in the transmission rate is added to the model (1)–(5) via a sine function with a period of 365

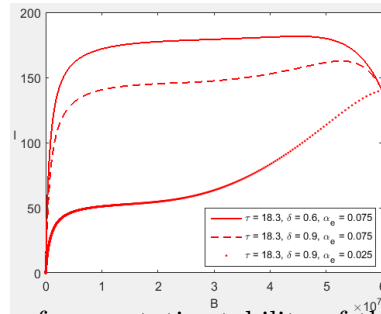


FIGURE 6. Confirmation of asymptotic stability of the disease-free equilibrium point of (1)–(5) when $\mathfrak{R}_0 < 1$

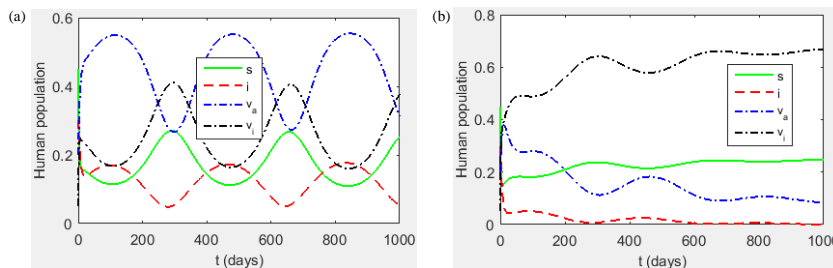


FIGURE 7. Solution of model (1)–(5) with seasonal variation in environment-to-human transmission rate.

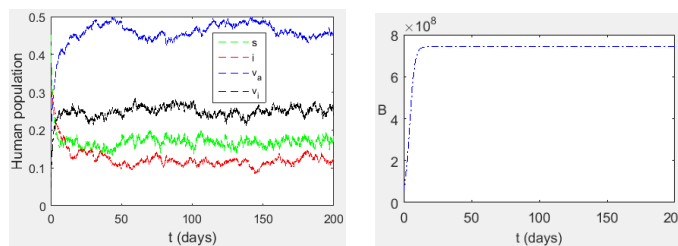


FIGURE 8. Simulation of model (13) using the parameter values in Table 1

days, ie

$$\alpha_e(t) = \alpha_e \left(1 + \alpha_0 \sin \left(\frac{2\pi t}{365} \right) \right),$$

where $0 \leq \alpha_0 \leq 1$ accounts for the seasonal variation. For our computation, we choose $\alpha_0 = 0.7$ and other parameters as contained in Table 1. Figure 10(a) shows that the oscillation in the environment-to-human transmission rate causes oscillation in the dynamics of the disease. However if we choose $\tau = 18.3$, $\delta = 0.9$ and $\alpha_e = 0.025$ such that $\mathfrak{R}_0 = 0.9935$, the oscillation dies out and the disease vanishes (see Figure 10(b)).

4.2. Stochastic Model. In this section, numerical solution of the model (13) is done using Euler-Maruyama scheme. Since this scheme is of low convergence rate, we pick $\Delta t = \frac{1}{2000}$. The parameter values in Table 1 are used for our computation.

It is obvious in Figure 8 that cholera is endemic in the population. Although the population of vaccinated and vigilant individuals is high, yet the disease remains in the system. It can also be seen that the effect of randomness on the human population does not affect the density of *Vibrio cholerae*.

Next, we consider (i) increase in disinfection rate (τ), (ii) improvement in public health education (δ) and (iii) provision of safe drinking water to reduce environment-to-human transmission rate (α_e) as intervention in stochastic setting. The parameter values $\tau = 18.3$, $\delta = 0.9$ and $\alpha_e = 0.025$ which are used to obtain Figure 5 are used to simulate (13). In Figure 9, the population of infected people first increases before decreasing due to the high density of *V. cholerae* in the environment. Vibrios density is seen to decrease while more people become vigilant and

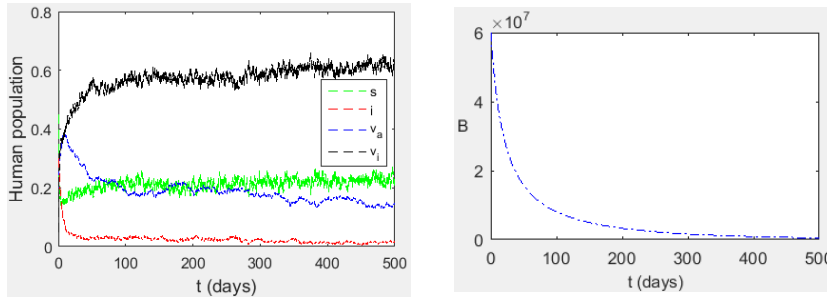


FIGURE 9. Simulation of model (13) taking $\tau = 18.3$, $\delta = 0.9$ and $\alpha_e = 0.025$ such that $\mathfrak{R}_0 = 0.9935$. Other parameter values are used as contained in Table 1

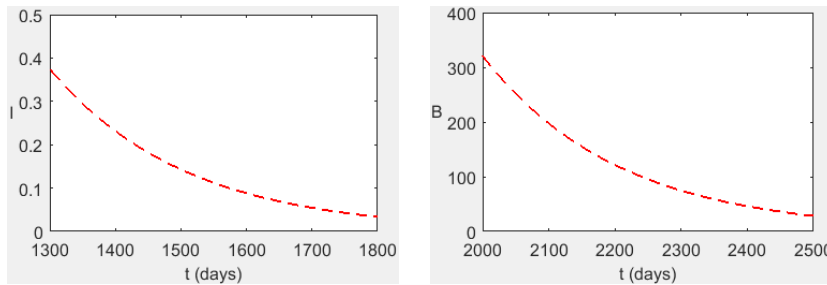


FIGURE 10. Simulation of model (1)–(5) taking $\tau = 18.3$, $\delta = 0.9$ and $\alpha_e = 0.025$ such that $\mathfrak{R}_0 = 0.9935$. Other parameter values are as contained in Table 1

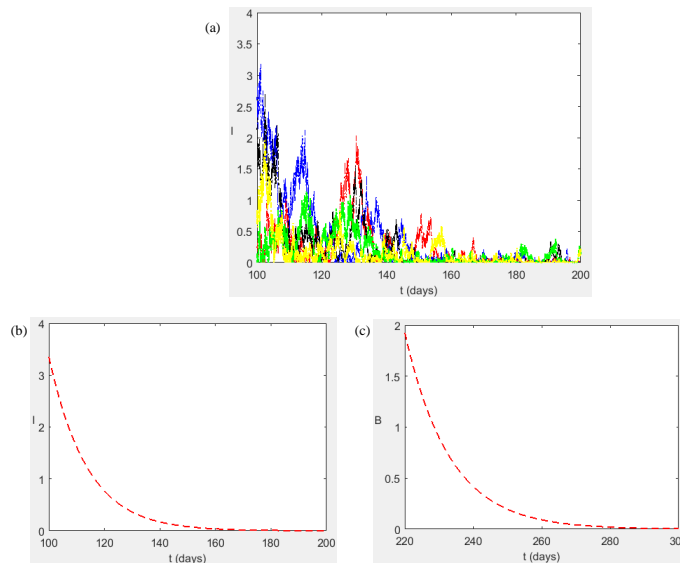


FIGURE 11. (a) Extinction of cholera with random effect (b) Extinction of cholera without random effect (c) Eradication of *Vibrio cholerae* in the environment

thereby reducing the efforts expended on vaccination. Thus, being vigilant could be of great impact in controlling the spread of cholera.

4.3. Extinction. The main objective in epidemiology is concerned with the regulation of the disease dynamics so that the disease will be eradicated from the population in the long term. Due to the types of entries in the diffusion matrix of (13) and considering the number of Wiener processes in relation to the number of equations, constructing a stochastic Lyapunov function is somewhat difficult and the method used in the previous articles [43, 44, 28] are not applicable. We therefore employ numerical means.

With the initiation of the intervention measures (such that $\mathfrak{R}_0 < 1$), it still takes an upward of 2500 days to eradicate the disease. To have a rapid decay in the disease classes, certain measures

must be implemented. Let B_0 be the amount of the *Vibrio cholerae* per ml before the initiation of the control measures, the disease will be eradicated by the end of t_0 days if

$$\mathfrak{R}_0 < 1, \quad \zeta = 0, \quad \text{and} \quad \tau \geq \frac{1}{\varpi} \left[\rho - \sigma + \frac{1}{t_0} (5 + \ln B_0) \right]. \quad (14)$$

Next we choose $t_0 = 300$ and τ, δ such that (14) is satisfied while other parameter values remain as contained in Table 1. To estimate the extinction time when there is random effect, we obtain many different sample paths for model (13). Figure 11 shows that all the solution paths of infected human class, $I(t)$, and *V. cholerae*, $B(t)$, decrease and become approximately zero before the 300 days.

5. CONCLUSION

We have considered a deterministic cholera model incorporating vigilant human class. The model was later extended to incorporate randomness following the approach presented in [29, Section 5.6]. With this approach, the diffusion coefficients depend on the parameters derived from the basic assumptions of the model and a better understanding of the influence of the parameters in the model is achieved. Condition that establish the global stability of the disease-free equilibrium point of the determinist model was given. With this condition, we simulate the stochastic model to understand the influence of randomness on the dynamics of the disease. The stochastic version of the deterministic cholera model is more realistic for cholera dynamics as it is widely open to some uncertain effects on the disease dynamics.

The focus of epidemiological study is to investigate and implement control and prevention measures. The use of cholera vaccines has been recognized as an effective control measure in cholera endemic countries [45] however, it was discovered that vaccination only is not sufficient for the eradication of cholera in an endemic setting. Improvement on public health education and provision of safe drinking water to reduce environment-to-human transmission rate are prerequisites for cholera control and eradication. Because *Vibrio cholerae* multiplies at a fast rate in the environment and based on (14), it is strongly recommended that environmental sanitation and regular disinfection of the affected area (i.e. sewage areas) be maintained. However, [46] reported that the use of disinfectant should be medically and scientifically monitored as increased risk of bladder cancer appeared to be associated with the consumption of chlorinated water. Numerical experiment is done to estimate the expected extinction time of the disease when certain conditions are met.

REFERENCES

- [1] Cholera vaccines: WHO position paper, *Wkly. Epidemiol. Rec.* 92 (34) (2017) 477–500.
<http://apps.who.int/iris/bitstream/10665/258763/1/WER9234.pdf?ua=1>
- [2] Sun, G. Q., Xie, J. H., Huang, S. H., Jin, Z., Li, M. T. and Liu, L., (2017), Transmission dynamics of cholera: mathematical modeling and control strategies, *Commun. Nonlinear, Sci. Numer. Simul.*, 45, pp. 235–244 .
- [3] Shuai, Z. and van den Driessche, P., (2011), Global dynamics of cholera models with differential infectivity, *Math. Biosci.*, 234 (2) pp. 118–126.
- [4] Scientific Committee on Enteric Infections and Foodborne Diseases, Epidemiology, prevention and control of cholera in Hong Kong, Center for Health Protection, Department of Health, Hong Kong Special Administrative Region (2011).
http://www.chp.gov.hk/files/pdf/epidemiology_prevention_and_control_of_cholera_in_hong_kong_r.pdf
- [5] Nelson, E. J., Harris, J. B., Glenn Morris Jr, J., Calderwood, S. B., and Camilli, A., (2009), Cholera transmission: the host, pathogen and bacteriophage dynamic, *Nature Reviews (Microbiology)* 7, pp. 693–702.
- [6] World Health Statistics 2016: Monitoring health for the SDGs.
https://www.who.int/gho/publications/world_health_statistics/2016/en/.
- [7] Media Centre, Cholera, World Health Organization, 2017.
<http://www.who.int/mediacentre/factsheets/fs107/en/>.
- [8] Graves, P. M., Deeks, J. J., Demicheli, V. and Jefferson, T., (2010), Vaccines for preventing cholera: killed whole cell or other subunit vaccines (injected), *Cochrane Database of Systematic Reviews* (8).
- [9] Sinclair, D., Abba, K., Zaman, K., Qadri, F. and Graves, P. M., (2011), Oral vaccines for preventing cholera, *Cochrane Database of Systematic Reviews* (3).

- [10] Posny, D., Wang, J., Mukandavire, Z. and Modnak, C., (2015) Analyzing transmission dynamics of cholera with public health interventions, *Math. Biosci.*, 264, pp. 38–53.
- [11] Mukandavire, Z., Liao, S., Wang, J., Gaff, H., Smith, D. L. and Morris, J. G. Jr, (2011), Estimating the reproductive numbers for the 2008-2009 cholera outbreaks in zimbabwe, *Proc Natl Acad Sci U S A*, 108 (21) pp. 8767–8772.
- [12] Beryl, M. O., George, L. O. and Fredrick, N. O., (2016), Mathematical analysis of a cholera transmission model incorporating media coverage, *Int. J. of Pure and Applied Mathematics*
- [13] Capone, F., De Cataldis, V. and De Luca, R., (2015), Influence of diffusion on the stability of equilibria in a reaction-diffusion system modeling cholera dynamic, *J. Math. Biol.* 71 (5), pp. 1107–1131.
- [14] Lemos-Paião, A. P., Silva, C. J. and Torres, D. F. M., (2017), An epidemic model for cholera with optimal control treatment, *J. Comput. Appl. Math.*, 318 pp. 168–180.
- [15] Kong, J. D., Davis, W. and Wang, H., (2014), Dynamics of a cholera transmission model with immunological threshold and natural phage control in reservoir, *Bull. Math. Biol.* 76 (8), pp. 2025–2051.
- [16] Lin, J., Xu, R. and Tian, X., (2019), Global dynamics of an age-structured cholera model with multiple transmissions, saturation incidence and imperfect vaccination, *J. Biol. Dyn.* 13 (1), pp. 69–102.
- [17] Lin, J., Xu, R. and Tian, X., (2018), Global dynamics of an age-structured cholera model with both human-to-human and environment-to-human transmissions and saturation incidence, *Appl. Math. Model.* 63 pp. 688–708.
- [18] Njagarah, J. B. H. and Nyabadza, F., (2014), A metapopulation model for cholera transmission dynamics between communities linked by migration, *Appl. Math. Comput.* 241, pp. 317–331 .
- [19] Ogunmiloro, O. M. and Ogunlade, T. O., (2019), Transmission dynamics of cholera epidemic model with latent and hygiene complaint class, *Electron. J. Math. Anal. Appl.* 7 (2), pp. 138–150 .
- [20] Wang, X., Chen, Y. and Song, X., (2019), Global dynamics of a cholera model with age structures and multiple transmission modes, *Int. J. Biomath.* 12 (5), 1950051, 34.
- [21] Yang, C., Posny, D., Bao, F. and Wang, J., (2018), A multi-scale cholera model linking between-host and within-host dynamics, *Int. J. Biomath.* 11 (3), 1850034, 23.
- [22] Wang, Y. and Cao, J., (2015), Global stability of general cholera models with nonlinear incidence and removal rates, *J. Franklin Inst.* 352 (6) pp. 2464–2485.
- [23] Wang, J., Xie, F. and Kuniya, T., (2020), Analysis of a reaction-diffusion cholera epidemic model in a spatially heterogeneous environment, *Commun. Nonlinear Sci. Numer. Simul.* 80, 104951, 20.
- [24] Faniran, T. S. and Adewole, M. O., (2022), Analysis of a cholera model with treatment noncompliance, *Int. J. Nonlinear Anal. Appl.* 13 (1), pp. 29–43.
- [25] Wang, X. and Wang, J., (2017), Modeling the within-host dynamics of cholera: bacterial-viral interaction, *J. Biol. Dyn.* 11 (suppl. 2), pp. 484–501.
- [26] Marwa, Y. M., Mbalawata, I. S., Mwalili, S. and Charles, W. M., (2019), Stochastic dynamics of cholera epidemic model: Formulation, analysis and numerical simulation, *Journal of Applied Mathematics and Physics* 7, pp. 1097–1125.
- [27] Rezaeyan, R. and Farnoosh, R., (2010), Stochastic differential equations and application of the Kalman-Bucy filter in the modeling of RC circuit, *Appl. Math. Sci. (Ruse)*, 4 (21-24), pp. 1119–1127.
- [28] Liu, Q., Jiang, D., Hayat, T. and Alsaedi, A., (2019), Dynamical behavior of a stochastic epidemic model for cholera, *J. Franklin Inst.* 356 (13), pp. 7486–7514.
- [29] Allen, E., (2007), Modeling with Itô stochastic differential equations, Vol. 22 of *Mathematical Modelling: Theory and Applications*, Springer, Dordrecht.
- [30] Mwasa, A. and Tchuente, J., (2011), Mathematical analysis of a cholera model with public health interventions, *BioSystems* 105, pp. 190–200.
- [31] World Health Organization (WHO), webpage: www.who.org.
- [32] Martinez, R. M., Megli, C. J. and Taylor, R. K., (2010), Growth and laboratory maintenance of vibrio cholerae, *Curr Protoc Microbiol.* (May; 0 6: Unit-6A.1), pp. 629–656.
- [33] Codeco, C. T., (2001), Endemic and epidemic dynamics of cholera: The role of the aquatic reservoir, *BMC Infectious Diseases* 1 (1).
- [34] Hartley, D. M., Morris, J. G., Jr and Smith, D. L., (2005), Hyperinfectivity: A critical element in the ability of *v. cholerae* to cause epidemics?, *PLOS Medicine* 3 (1).
- [35] Diekmann, O., Heesterbeek, J. A. P. and Metz, J. A. J., (1990), On the definition and the computation of the basic reproduction ratio R_0 in models for infectious diseases in heterogeneous populations, *J. Math. Biol.* 28 (4), pp. 365–382.
- [36] van den Driessche, P. and Watmough, J., (2002), Reproduction numbers and sub-threshold endemic equilibria for compartmental models of disease transmission, *Math. Biosci.* 180, pp. 29–48. John A. Jacquez memorial volume.
- [37] Castillo-Chavez, C., Feng, Z. and Huang, W., (2002), On the computation of R_0 and its role on global stability, in: *Mathematical approaches for emerging and reemerging infectious diseases: an introduction* (Minneapolis, MN, 1999), Vol. 125 of *IMA Vol. Math. Appl.*, Springer, New York, 2002, pp. 229–250.
- [38] Wang, J. and Liao, S., (2012), A generalized cholera model and epidemic-endemic analysis, *J. Biol. Dyn.* 6 (2), pp. 568–589.

- [39] Allen, L. J. S., (2008), An introduction to stochastic epidemic models, in: *Mathematical epidemiology*, Vol. 1945 of *Lecture Notes in Math.*, Springer, Berlin, pp. 81–130.
- [40] Mao, X., (2008), *Stochastic differential equations and applications*, 2nd Edition, Horwood Publishing Limited, Chichester.
- [41] Khan, T., Jung, I. H. and Zaman, G., (2019), A stochastic model for the transmission dynamics of hepatitis B virus, *J. Biol. Dyn.* 13 (1), pp. 328–344.
- [42] Hartley, D. M., Morris, J. G. and Smith, D. L., (2006), Hyperinfectivity: a critical element in the ability of *v. cholerae* to cause epidemics?, *Plos Med.*, 3.
- [43] Khan, T., Khan, A. and Zaman, G., (2018), The extinction and persistence of the stochastic hepatitis B epidemic model, *Chaos Solitons and Fractals*, 108, pp. 123–128.
- [44] Liu, Q., Jiang, D., Shi, N., Hayat, T. and Alsaedi, A., (2017), Stationary distribution and extinction of a stochastic SIRS epidemic model with standard incidence, *Phys. A* 469, pp. 510–517.
- [45] Modnak, C., (2017), A model of cholera transmission with hyperinfectivity and its optimal vaccination control, *Int. J. Biomath.* 10 (6), 1750084, 16.
- [46] Cantor, K. P., Hoover, R., Hartge, P., Mason, T. J., Silverman, D. T., Altman, R., Austin, D. F., Child, M. A., Key, C. R., Marrett, L. D., Myers, M. H., Narayana, A. S., Levin, L. I., Sullivan, J. W., Swanson, G. M., Thomas, D. B. and West., W. D., Bladder cancer, drinking water source and tap water consumption: a casecontrol study, *Journal of the National Cancer Institute* 79, pp. 1269–1279.



Matthew O. Adewole had his undergraduate study at Ladoke Akintola University of Technology and his postgraduate studies at the University of Ibadan, Nigeria. He is also interested in capturing real-life situations using models involving fractional differential equations and partial differential equations.



Prof. Izani obtained his undergraduate and postgraduate degrees from the UK. He has been with Universiti Sains Malaysia (USM) since 1984 and was conferred his Professorship in 2011.



Assoc. Prof. Dr. Farah Aini completed her PhD in Computational Mathematics at the University of Queensland in 2009. Since her graduation, she has worked in computational and applied mathematics at School of Mathematics, USM. Dr Farah's main research interests are in the fields of Computational Mathematics, Computational Biology and Fractional Differential Modelling.



Taye Samuel Faniran obtained his Ph.D. degree in Mathematics from University of Ibadan, Nigeria. His research areas are mathematical modeling of infectious diseases and computational mathematics.

Appendix A. Construction of the stochastic model (13)

For a small time step Δt , let the probabilities of the changes within the states be $p_j(t, \mathbf{X}(t))\Delta t$ for $j = 1, 2, \dots, n$. Here the j th change modifies the i th state by an amount λ_{ji} for $i = 1, 2, \dots, d$. A standard deterministic model is given in form of system of ODEs as

$$d\mathbf{X} = \mathbf{f}(t, \mathbf{X}(t)) dt.$$

The i th element of the vector \mathbf{f} is

$$f_i(t, \mathbf{X}(t)) = \sum_{j=1}^n p_j(t, \mathbf{X}(t))\lambda_{ji}, \quad i = 1, 2, \dots, d.$$

Following [29, Section 5.6], randomness is incorporated using

$$X_i^{r+1} - X_i^r = \sum_{j=1}^n p_j(t, \mathbf{X}^r(t))\lambda_{ji}\Delta t + \sum_{j=1}^n \lambda_{ji}[p_j(t, \mathbf{X}^r(t))]^{1/2}(\Delta t)^{1/2}\sigma_j, \quad i = 1, \dots, d, \quad r = 1, 2, \dots, \quad (15)$$

where $\sigma_j \sim N(0, 1)$. We therefore obtain the following discrete model

$$\begin{aligned} S^{r+1} - S^r &= \left[\Lambda - \left(\alpha_h I^r + \alpha_e \frac{B^r}{\mathcal{K} + B^r} \right) S^r - (\mu + \beta + \psi)S^r + \omega V_a^r + \xi V_i^r \right] \Delta t + \left[\sqrt{\Lambda} \sigma_1 \right. \\ &\quad \left. - \sqrt{\left(\alpha_h I^r + \alpha_e \frac{B^r}{\mathcal{K} + B^r} \right) S^r} \sigma_2 - \sqrt{\mu S^r} \sigma_3 - \sqrt{\beta S^r} \sigma_4 - \sqrt{\psi S^r} \sigma_5 + \sqrt{\omega V_a^r} \sigma_6 + \sqrt{\xi V_i^r} \sigma_7 \right] \sqrt{\Delta t} \quad (16) \\ I^{r+1} - I^r &= \left[\left(\alpha_h I^r + \alpha_e \frac{B^r}{\mathcal{K} + B^r} \right) ((1 - \eta)V_a^r + S^r) - (\mu + \gamma \kappa)I^r \right] \Delta t \\ &\quad + \left[\sqrt{\left(\alpha_h I^r + \alpha_e \frac{B^r}{\mathcal{K} + B^r} \right) S^r} \sigma_2 - \sqrt{\mu I^r} \sigma_{10} + \sqrt{\left(\alpha_h I^r + \alpha_e \frac{B^r}{\mathcal{K} + B^r} \right) (1 - \eta)V_a^r} \sigma_8 - \sqrt{\gamma \kappa I^r} \sigma_9 \right] \sqrt{\Delta t} \\ V_a^{r+1} - V_a^r &= \left[\beta S^r + \gamma \kappa I^r - (\omega + \mu)V_a^r - (1 - \eta) \left(\alpha_h I^r + \alpha_e \frac{B^r}{\mathcal{K} + B^r} \right) V_a^r \right] \Delta t \\ &\quad + \left[-\sqrt{\mu V_a^r} \sigma_{11} + \sqrt{\beta S^r} \sigma_4 - \sqrt{\left(\alpha_h I^r + \alpha_e \frac{B^r}{\mathcal{K} + B^r} \right) (1 - \eta)V_a^r} \sigma_8 + \sqrt{\gamma \kappa I^r} \sigma_9 \right] \sqrt{\Delta t} \\ V_i^{r+1} - V_i^r &= [\psi S^r - (\xi + \mu)V_i^r] \Delta t + \left[-\sqrt{\mu V_i^r} \sigma_{12} + \sqrt{\psi S^r} \sigma_5 - \sqrt{\xi V_i^r} \sigma_7 \right] \sqrt{\Delta t}. \quad (17) \end{aligned}$$

As $\Delta t \rightarrow 0$, the discrete model (16)–(17) becomes

$$\begin{aligned} dS &= \left[\Lambda - \left(\alpha_h I + \alpha_e \frac{B}{\mathcal{K} + B} \right) S - (\mu + \beta + \psi)S + \omega V_a + \xi V_i \right] dt + \sqrt{\Lambda} dW_t^1 - \sqrt{\left(\alpha_h I + \alpha_e \frac{B}{\mathcal{K} + B} \right) S} dW_t^2 \\ &\quad - \sqrt{\mu S} dW_t^3 - \sqrt{\beta S} dW_t^4 - \sqrt{\psi S} dW_t^5 + \sqrt{\omega V_a} dW_t^6 + \sqrt{\xi V_i} dW_t^7 \quad (18) \\ dI &= \left[\left(\alpha_h I + \alpha_e \frac{B}{\mathcal{K} + B} \right) ((1 - \eta)V_a + S) - (\mu + \gamma \kappa)I \right] dt + \sqrt{\left(\alpha_h I + \alpha_e \frac{B}{\mathcal{K} + B} \right) S} dW_t^2 - \sqrt{\mu I} dW_t^{10} \\ &\quad + \sqrt{\left(\alpha_h I + \alpha_e \frac{B}{\mathcal{K} + B} \right) (1 - \eta)V_a} dW_t^8 - \sqrt{\gamma \kappa I} dW_t^9 \\ dV_a &= \left[\beta S + \gamma \kappa I - (\omega + \mu)V_a - (1 - \eta) \left(\alpha_h I + \alpha_e \frac{B}{\mathcal{K} + B} \right) V_a \right] dt - \sqrt{\mu V_a} dW_t^{11} + \sqrt{\beta S} dW_t^4 \\ &\quad - \sqrt{\left(\alpha_h I + \alpha_e \frac{B}{\mathcal{K} + B} \right) (1 - \eta)V_a} dW_t^8 + \sqrt{\gamma \kappa I} dW_t^9 \\ dV_i &= [\psi S - (\xi + \mu)V_i] dt - \sqrt{\mu V_i} dW_t^{12} + \sqrt{\psi S} dW_t^5 - \sqrt{\xi V_i} dW_t^7. \quad (19) \end{aligned}$$

Although this method yields a SDEs which are generally easy to solve, model (16)–(17) loses much of its computational advantages when the number of Weiner processes is much greater than the number of states. We therefore assume that the natural death rate of state variables have the same probability distribution ie. $\sigma_3 = \sigma_{10} = \sigma_{11} = \sigma_{12}$. This leads to (13).